

# Sodium Passivation of the Grain Boundaries in $\text{CuInSe}_2$ and $\text{Cu}_2\text{ZnSnS}_4$ for High-Efficiency Solar Cells

Cheng-Yan Liu, Zhi-Ming Li, Hong-Yang Gu, Shi-You Chen, Hongjun Xiang, and Xin-Gao Gong\*

It is well known that sodium at grain boundaries (GBs) increases the photovoltaic efficiencies of  $\text{CuInSe}_2$  and  $\text{Cu}_2\text{ZnSnS}_4$  significantly. However, the mechanism of how sodium influences the GBs is still unknown. Based on the recently proposed self-passivation rule, it is found that the dangling bonds in the GBs can completely be saturated through doping the Na, thus GB states are successfully passivated. It is shown that the Na can easily incorporate into the GB with very low formation energy. Although Cu can also passivate the GB states, it requires a copper rich condition which, however, suppresses the formation of copper vacancies in the bulk and thus decreases the concentration of hole carriers, so copper passivation is practically not as beneficial as sodium. The present work reveals the mechanism about how the Na enhances the photovoltaic performance through passivating the dangling bonds in the GBs of chalcogenide semiconductors, and sheds light on how to passivate dangling bonds in GBs with alternative processes.

## 1. Introduction

Alkaline metals incorporating in  $\text{Cu}(\text{In}, \text{Ga})\text{Se}_2$  (CIGSe)<sup>[1–6]</sup> and  $\text{Cu}_2\text{ZnSnS}_4$  (CZTS)<sup>[7–10]</sup> have experimentally shown significant improvement in photovoltaic efficiencies. As sodium treatment technology advances, such as postdeposition treatment,<sup>[2]</sup> soda-lime glass substrate,<sup>[11,12]</sup> and Na in Mo back contacts,<sup>[13–15]</sup> solar cells' efficiencies have risen to 22.6% for CIGS<sup>[5]</sup> and 12.6% for CZTS.<sup>[16]</sup> However, despite decades of investigations,<sup>[17–22]</sup> the reason for success of sodium treatment is still a mystery. Experiments observed that Na predominantly segregates at grain boundaries (GBs) or interfaces,<sup>[22,23]</sup> which typically acted as nonradiative recombination centers.<sup>[24–28]</sup> These indicate that

Na in GBs plays an important role in the improvement of solar cells efficiencies.

Up to now, there was no self-consistent explanation of the role of Na in GBs. Previous experiments suggested that Na increased grain size with a reduction of intragranular lattice defects leaving residual Na in GBs.<sup>[17–19]</sup> Also induced surface dipoles reduced the work function, resulting in high local built-in potential in GBs<sup>[21]</sup> and led to a high electrical potential at GBs which could enhance carrier separation.<sup>[22]</sup> However, there was other evidence that Na resulted in reduced grain size during growth of thin films<sup>[2]</sup> and without Na incorporation, GBs also display high built-in potential in GBs.<sup>[20]</sup> Extensive theoretical studies indicated that these GBs indeed caused large numbers of defect states stemming from anion-core

wrong bonds.<sup>[24,25]</sup> In order to eliminate these defect states, some complex engineering doping approaches were proposed to passivate the defect states through breaking or weakening the wrong bonds which produce these defect states, such as  $\text{Cu}_{\text{In}}$  and  $\text{O}_{\text{Se}}$  at  $\text{CuInSe}_2$  (CISE) GBs<sup>[26]</sup> and  $\text{Zn}_{\text{Sn}}+\text{O}_{\text{Se}}+\text{Na}^+$  copassivation for CZTSe GBs.<sup>[27]</sup> These theoretical studies have nothing to do with the effect of Na incorporation. In fact, Na substituting cations (Cu and In) can not affect the anion pairs' wrong bonds, so it would not be expected that the above doping approaches would improve the GB properties. Theoretical studies on Na incorporating in the bulk of chalcogenide semiconductors are still struggling with interior grain defects, such as producing acceptor energy states with  $\text{Na}_{\text{In}_{\text{Ga}}}$  and  $\text{Na}_{\text{In}_{\text{Cu}}}$ <sup>[29]</sup> in CIGSe films and inducing energy band shifting, broadening, and narrowing in CZTS films.<sup>[30]</sup> These studies revealed that Na eliminating  $\text{In}_{\text{Cu}}$  and  $\text{In}_{\text{Ga}}$  defects can increase the p-type carriers, which are crucial for photocurrent in these materials.<sup>[29,30]</sup> However, Na was also believed to replace the acceptor  $V_{\text{Cu}}$  in CIGSe<sup>[31]</sup> and decreases the optical absorption band gap in CZTS.<sup>[30]</sup>

In this work, we study the electronic properties of CISE and CZTS anion-core prototype  $\Sigma 3$  (114) GB<sup>[28,32]</sup> and Na (Cu) doping. Combining with the recently proposed self-passivation rule<sup>[33]</sup> with the first-principles calculations, we find that Cu can effectively passivate the GBs' defect states under Cu rich conditions, but such conditions were seldom used because they suppress the formation of the desired Cu vacancies. The same passivation rule applied to Na doping not only can obtain better passivating effects, but also has a lower formation energy

Dr. C.-Y. Liu, Z.-M. Li, H.-Y. Gu, Prof. H. Xiang, X.-G. Gong  
Key Laboratory for Computational  
Physical Science (Ministry of Education)  
State Key Laboratory of Surface Physics  
and Department of Physics  
Fudan University  
Shanghai 200433, China  
E-mail: xggong@fudan.edu.cn

Dr. C.-Y. Liu, Z.-M. Li, H.-Y. Gu, Prof. H. Xiang, X.-G. Gong  
Collaborative Innovation Center of Advanced Microstructures  
Nanjing 210093, Jiangsu, China

Prof. S.-Y. Chen  
Laboratory of Polar Materials and Devices  
East China Normal University  
Shanghai 200241, China

DOI: 10.1002/aenm.201601457



than that of Cu doping. Therefore, we provide a mechanism for why Na treatment is crucial for achieving *p*-type samples under Cu poor conditions in multicompositional chalcogenide semiconductors.

## 2. Simulation Methodology

### 2.1. Grain Boundary Passivation Model

For polycrystalline semiconductors, unpaired electrons in surfaces or interfaces forming dangling bonds or wrong bonds are usually detrimental to photovoltaic performance by creating defect states in the band gap.<sup>[24–27,33]</sup> Generally, octet electron counting (OEC) rule realized by edge reconstruction,<sup>[34,35]</sup> surface reconstructions,<sup>[36,37]</sup> and external atoms passivation<sup>[38]</sup> has been successfully used in passivating the unpaired electrons in most of the covalent semiconductors. Considering the unpaired electrons saturating mechanism, we recently proposed a GB self-passivation rule which has been successfully applied to find the reconstruction GBs with benign electronic properties in CdTe.<sup>[33]</sup> Since the binary zinc-blende structure (CdTe), ternary chalcopyrite structure (CISe), and quaternary kesterite structure (CZTS) are a series of tetrahedral compounds through cation mutation, the self-passivation rule should also be suitable for CISe and CZTS systems to eliminate defect states.

Based on the self-passivation rule,<sup>[33]</sup> we propose a saturating mechanism of unpaired electrons in anion-core  $\Sigma 3$  (114) GB of CISe and CZTS. In a perfect CISe crystal, each Se atom gets a filled outer shell through obtaining  $2 \times 0.25$  fractional electron from two nearest neighbor Cu ions and  $2 \times 0.75$  fractional electrons from two nearest neighbor In ions. However, at the anion-core GB region, full-shell states are destroyed near the core, leaving two Se1 dangling bonds with  $0.75 e$  deficiency (absenting two In atoms) and two Se2 dangling bonds with  $0.25 e$  deficiency (absenting two Cu atoms) as shown in Figure 1a. This leads to two electrons missing in the GB unit cell. Therefore, adding two electrons by inserting two extra monovalent

atoms or one divalent atom can satisfy the OEC rule as shown in Figure 1a (inset). Similarly, this saturation mechanism is also suitable for CZTS GB. In a perfect CZTS crystal, each S atom accepts  $2 \times 0.25$  fractional electron from two nearest neighbor Cu ions,  $0.5$  fractional electron from one nearest neighbor Zn ion and  $1.0$  electron from one nearest neighbor Sn ion. At the CZTS GB region, full-shell states are broken, leaving two S1 dangling bonds with  $0.50 e$  deficiency (absenting two Zn atoms) and two S2 dangling bonds with  $0.25 e$  deficiency (absenting two Cu atoms) at the GB core as shown in Figure 1b. Thus, there is a  $1.5$  electron deficiency in per GB unit cell. Therefore, it is necessary to add three extra monovalent atoms to saturate all unpaired electrons in the double cells of GB as shown in Figure 1b (inset). This GB passivation model, which eliminates all dangling bonds, is expected to result in benign electronic properties and low formation energies in multicompositional chalcogenide semiconductors.

### 2.2. GB Models and First-Principles Calculations Method

The first-principles calculations were performed based on density functional theory with Vienna Ab Initio Simulation Package.<sup>[39,40]</sup> The projector-augmented wave method with Perdew–Burke–Ernzerhof functional<sup>[41]</sup> was used to calculate the formation energy in the simulations. We used Hubbard  $U = 6.0$  eV on the cation 3d orbital,<sup>[42,43]</sup> which leads to a band gap of  $0.48$  eV in bulk CISe<sup>[26]</sup> and  $0.61$  eV in bulk CZTS.<sup>[27]</sup> Since two different indispensable GBs contained in one supercell will inevitably lead to polarization, a slab of 43 layers with  $15 \text{ \AA}$  of vacuum was used to construct the slabs of  $\Sigma 3$  (114) unit cell CISe GB and double cells CZTS GB. Surfaces dangling bonds were passivated with pseudohydrogen atoms to mimic the bulk properties.<sup>[38]</sup> The models are fully relaxed with Hellmann–Feynman forces less than  $0.05$  eV  $\text{\AA}^{-1}$ . The energy cutoffs are  $350$  and  $400$  eV and the  $k$  points are sampled with a  $5 \times 4 \times 1$  and a  $4 \times 4 \times 1$  mesh in the Brillouin zone<sup>[44]</sup> for CISe and CZTS GB systems, respectively. In order to estimate

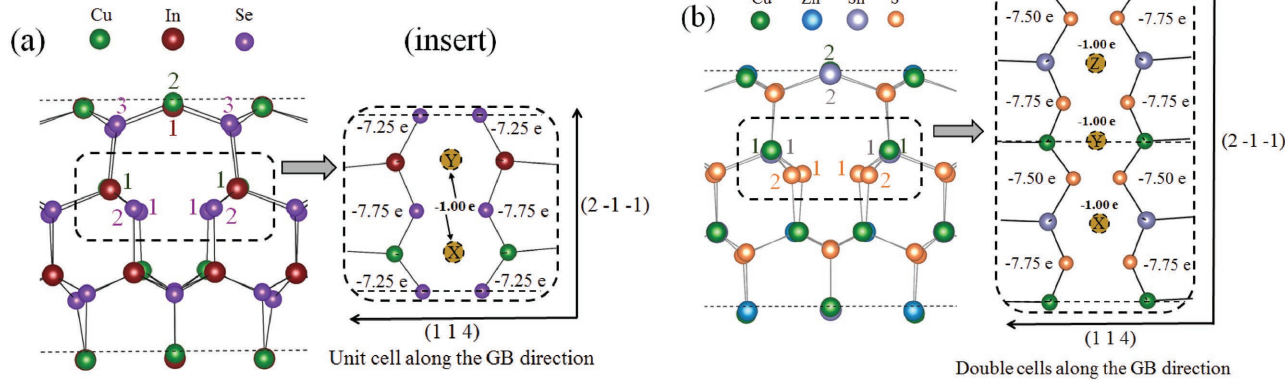


**Figure 1.** The schematic structure of anion-core  $\Sigma 3$  (114) GBs: a) for CISe and b) for CZTS. The number of valence electrons of anions is shown in the insets, which suggests that there are two electron and three electron deficiencies per unit cell of CISe GB and double cells of CZTS GBs, respectively. Thus, these dangling bonds can be saturated by adding two electrons in X and Y positions for CISe GB and three electrons in X, Y, and Z positions for CZTS GB. The atoms colored green, dark red, purple, blue, grey, and orange represent Cu, In, Se, Zn, Sn, and S, respectively.

the effects of quantum confinement, we construct the slab models with the same size of the GBs model, and find that the calculated band gaps are only 0.08 and 0.09 eV larger than the bulk systems of CISe and CZTS, respectively. This indicates that the quantum confinement effect is negligible.

### 3. Results and Discussion

#### 3.1. CISe GB with Cu and Na Incorporation

Based on the self-passivation rule, we studied the electronic structures of Cu and Na doped GBs comparing with the prototype GB of CISe. The band structures and local density of states (LDOS) of the prototype GB are shown in Figure 2a. It is clearly shown that the prototype CISe GB creates three localized defect energy levels marked with red circles in the band gap, which is consistent with the previous theoretical study.<sup>[26]</sup> The LDOS in Figure 2a shows that one unoccupied defect level is mainly derived from 4p–4p antibonding states of the Se<sub>1</sub>–Se<sub>1</sub> wrong bond (bond length 2.79 Å). Two other occupied defect levels are mainly derived from 4p–4p antibonding states of the Se<sub>2</sub>–Se<sub>2</sub> wrong bond (bond length 3.26 Å) and 5p–4s antibonding state of In<sub>1</sub>–Cu<sub>2</sub> wrong bond (bond length 2.64 Å). Since the hybridization coupling of Se<sub>1</sub>–Se<sub>1</sub> dimer with shorter bond length is stronger than that of the Se<sub>2</sub>–Se<sub>2</sub> dimer, the defect energy level originating from Se<sub>1</sub>–Se<sub>1</sub> 4p–4p antibonding state has higher energy.

Doping one electron in CISe GB cannot entirely satisfy GB passivation model. Taking NaX<sub>i</sub> and CuX<sub>i</sub> as examples, whose electronic properties are shown in Figure S2b,e (see the Supporting Information), respectively. The defect levels caused by Se<sub>2</sub>–Se<sub>2</sub> and Se<sub>1</sub>–Se<sub>1</sub> antibonding states move down to the Fermi energy level, just leaving a few shallow defect states above the Fermi energy level comparing with that of prototype GB shown in Figure 2a. The reason is that in NaX<sub>i</sub> and CuX<sub>i</sub>, Se–Se wrong bonds with higher energy of 4p–4p states are replaced by Se–Na or Se–Cu bonds with lower energy of 4p–3s (4p–4s) states. From the view of electron charge sharing, two Se<sub>2</sub> atoms with 2 × 7.75 e are saturated by capturing 2 × 0.25 e from Na or Cu and thus fill the shell, but two Se<sub>1</sub> atoms with 2 × 7.25 e capturing the residual 2 × 0.25 e from Na or Cu are not completely saturated. Therefore, the defect levels produced by Se<sub>1</sub>–Se<sub>1</sub> and Se<sub>2</sub>–Se<sub>2</sub> move to the bottom of valence band, leaving a few of shallow defect levels originating from Se<sub>1</sub>–Se<sub>1</sub> antibonding

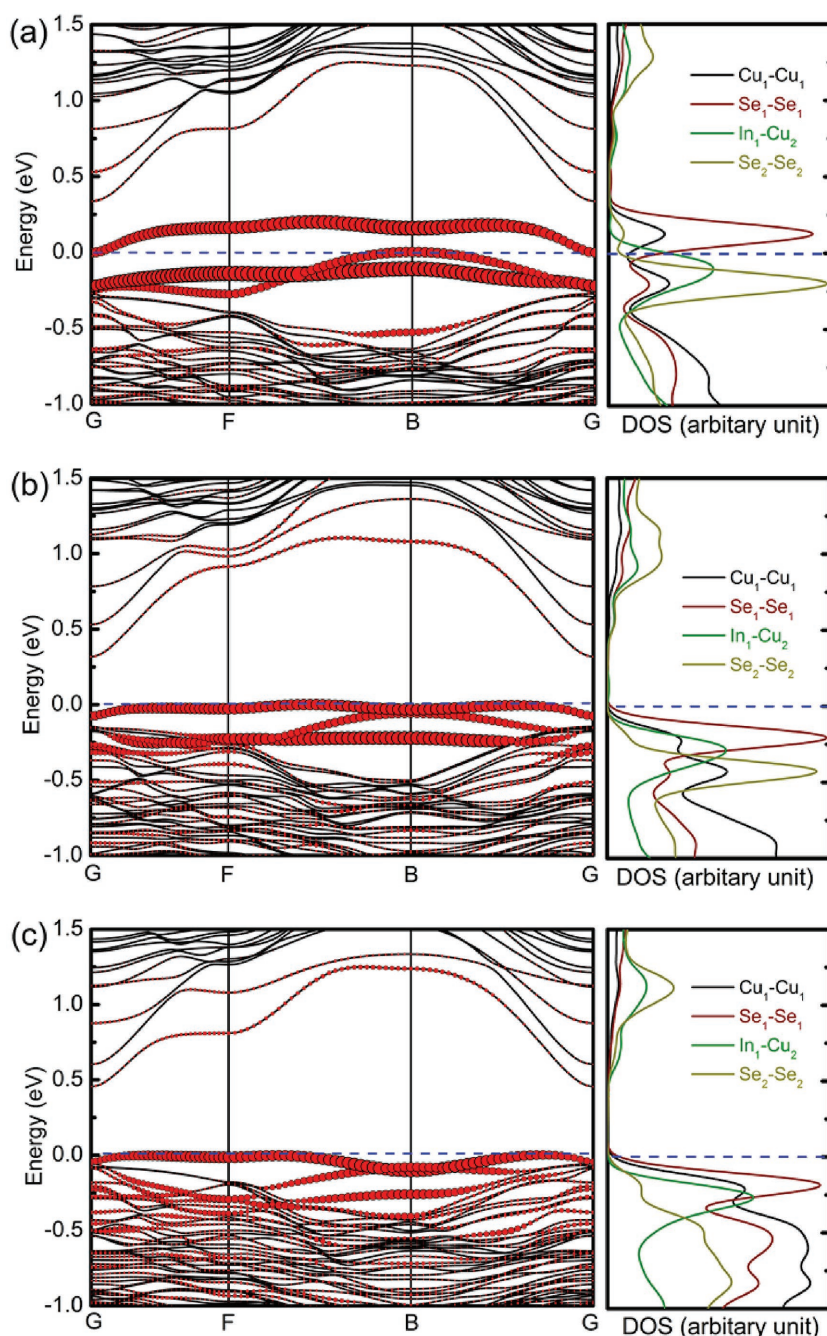


**Figure 2.** Band structures and local density of states (LDOS) of the CISe GB: a) Prototype GB, b) 2CuX,Y i, and c) 2NaX,Y i. The red circles represent the proportion of electron states contributing from the atoms at GB and the bigger the red circles are, the more they contribute to the energy bands (this description is also applied to the energy bands in Figure 5). Both 2CuX,Y i and 2NaX,Y i satisfying the passivation rule show benign electronic properties, in which the defect states originating from the different types of atoms shift down to the Fermi energy level.

states. The same mechanism is also suitable for the situation of NaY<sub>i</sub> (Y labeled in Figure 1a inset) whose electronic properties are shown in Figure S2c (see the Supporting Information).

When all the unpaired electrons of anions are saturated, the GB defect states can be completely removed from the band gap. For saturated 2CuX,Y i and 2NaX,Y i, the electronic properties

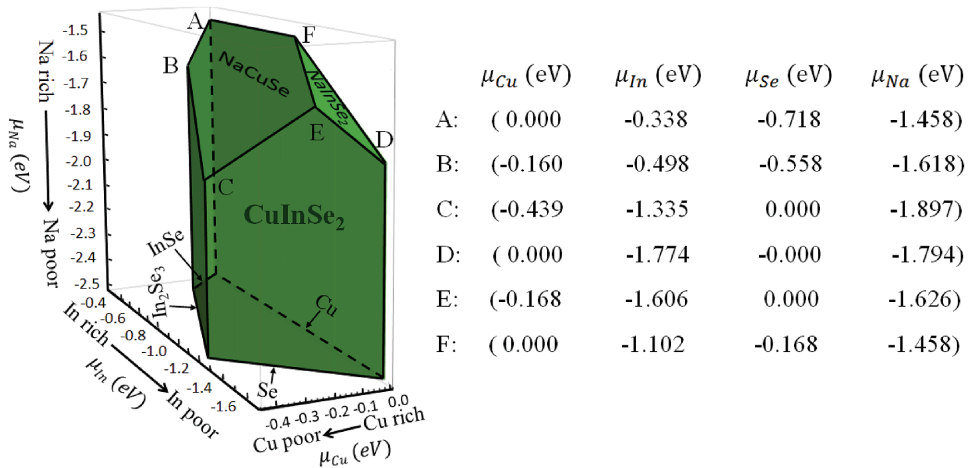


**Figure 3.** The calculated stable chemical potential region of CISe phase diagram with sodium incorporation. The corresponding coordinates for the upper limitation of richest Na chemical potential are the points A, B, C, D, E, and F as shown in the right of the figure.

are shown in Figure 2b and 2c, respectively. We can see that the defect states caused by wrong bonds of the GB are completely removed and leave a clean band gap. The reason is that  $2\text{Cu}_i\text{X}_i\text{Y}_i$  or  $2\text{Na}_i\text{X}_i\text{Y}_i$  provides two electrons at positions of X and Y resulting in two pairs of Se–Se 4p–4p dimers replaced by Se–Cu or Se–Na (4p–4s or 4p–3s) bonds, which satisfy the full-shell rule. Since the antibonding states Se–Cu or Se–Na (4p–4s or 4p–3s) have lower energy levels than these of Se–Se (4p–4p) antibonding states, the defect levels caused by GB unpaired electrons all lower to the Fermi energy level. Since Cu rich condition is usually avoided to increase the concentration of Cu vacancies and thus the hole carriers in these materials, Cu doped self-passivation GB is not popular. Therefore, Na post-treatment is a way to passivate the GB defect states with lower formation energy than that of Cu passivation, which is confirmed by the following formation energy calculation. Besides, other types of atoms, such as Ca treatment,<sup>[19]</sup> can also be used to passivate the GB defect states as long as the passivation rule is satisfied. Electronic structures (see Figure S4, Supporting Information) show that one Ca doping has the same passivating effect as  $2\text{Cu}_i$  and  $2\text{Na}_i$ , since all the three types of incorporations providing two electrons satisfy the passivation rule. Comparing the formation energies of  $\text{Ca}_i$ ,  $2\text{Na}_i$ , and  $2\text{Cu}_i$  in CISe GB (see Figure S5, Supporting Information), we find that  $\text{Ca}_i$  formation energy is slightly higher than  $2\text{Na}_i$ , but lower than  $2\text{Cu}_i$ . So Ca doping is a possible method under Cu poor condition to replace Na doping.

### 3.2. Formation Energies of CISe Doped GBs

The formation energy of dopants represents the stability of the doped structures. The lower the formation energy, the more stable the structure. The relative formation energy  $\Delta H_f$ <sup>[45,46]</sup> with the Na and Cu incorporated in CISe prototype GB is defined as

$$\Delta H_f = \Delta E + n_{Cu}\mu_{Cu} + n_{In}\mu_{In} + n_{Se}\mu_{Se} + n_{Na}\mu_{Na} \quad (1)$$

$$\begin{aligned} \Delta E = & E(\text{defect}_{\text{GB}}) - E(\text{prototype}_{\text{GB}}) \\ & + n_{Cu}\mu_{Cu}^0 + n_{In}\mu_{In}^0 + n_{Se}\mu_{Se}^0 + n_{Na}\mu_{Na}^0 \end{aligned} \quad (2)$$

where  $E(\text{prototype}_{\text{GB}})$  is the total energy of prototype GB, which is set as the reference,  $E(\text{defect}_{\text{GB}})$  is the total energy of the prototype GB doped with Cu, In, Se, or Na.  $n_{Cu}$ ,  $n_{In}$ ,  $n_{Se}$ , and  $n_{Na}$  are the numbers of Cu, In, Se, and Na atoms referring to the prototype GB.  $\mu_{Cu}$ ,  $\mu_{In}$ ,  $\mu_{Se}$ , and  $\mu_{Na}$  are the chemical potentials of Cu, In, Se, and Na relative to the chemical potentials  $\mu_{Cu}^0$ ,  $\mu_{In}^0$ ,  $\mu_{Se}^0$ , and  $\mu_{Na}^0$  of their elemental phases.

Based on the chemical potential conditions described in the Supporting Information, we obtain the  $\text{CuInSe}_2$  stable phase region limited by the chemical potential ranges of the constituted elements as shown in Figure 3. The richest Na chemical potential region is limited by the intersection points of A, B, C, D, E, and F, whose coordinates are listed in the right of the figure.

Therefore, formation energies of CISe GBs doped with Na and Cu in X and Y positions (shown in Figure 1a inset) at the different chemical potentials (A, B, C, D, E, and F) with Na richest condition can be obtained based on Equations (1) and (2). Figure 4 shows the formation energies of the doped GBs as a function of the chemical potentials (these values are listed in Table S1, Supporting Information). The fully relaxed atomic structures of these nine doped GBs are shown in Figure S1 (Supporting Information) and their corresponding electronic properties are shown in Figure S2 (Supporting Information).

Sodium as  $\text{NaX}_i$ ,  $2\text{Na}_i\text{X}_i\text{Y}_i$ , and  $\text{NaY}_i$  segregating at the CISe GB has lower formation energies than Cu related incorporations (Figure 4). Especially, Na in the X position ( $\text{NaX}_i$ ) displays lower formation energy than that of prototype GB in almost all the chemical potential region. Here, we find that single Na doping in X position has lower formation energy than doping in Y position. This is because an In ion at the top of the X position provides sufficient electrons to the bottom Se ion, so Na in the X position tends to be present in a larger space above the anion-core. Oppositely, Na in Y position should provide an electron to the bottom Se atom, which cannot obtain

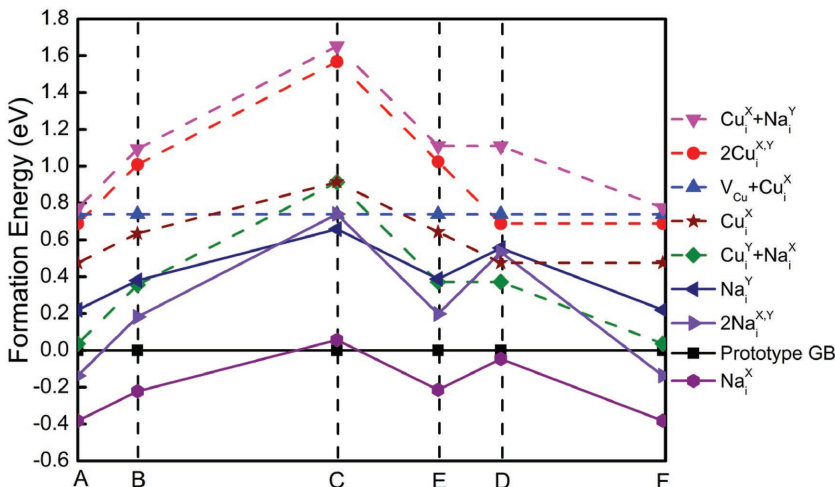


**Figure 4.** The formation energies of anion-core GB structures doped with Na and Cu at the selected points of the Na richest condition in the stable chemical potential region (Figure 3). Sodium incorporations as well as prototype GB are labeled by solid lines and Cu related incorporations are labeled by dashed lines. Na incorporated GBs do not only have lower formation energies than Cu related incorporations, but also spontaneously segregate at GBs with negative formation energies.

sufficient electrons from Cu atoms at the top of Y position. Also, 2NaX,Y i exhibits more stable structure than the prototype GB in the chemical potential regions of A and F. These indicate that Na spontaneously segregates at the GBs of chalcogenide semiconductor compounds, which is consistent with experimental observations.<sup>[22,23]</sup> In contrast, all forms involving Cu incorporations (2CuX,Y i, V<sub>Cu</sub>+CuX i, CuX i+NaY i, CuY i+NaX i, CuX i) have relatively higher formation energies than that of prototype GB. It is worth noting that these positions in the chemical potential region, except for C, are Cu rich condition. Consistent with the experimental observation, CISe near the GBs is not Cu rich, while the grain interiors are nearly stoichiometric.<sup>[47]</sup> Meanwhile, our calculations demonstrate that the formation energy of Na doping in GB is 1.65 eV lower than in tetrahedron vacancy of grain interiors. Therefore, Na is energetically more favorable to segregate into the GBs than in bulk region. These results verified that growing thin films with Cu poor condition<sup>[48,49]</sup> creates the desired p-type crystal with V<sub>Cu</sub> and appropriate proportion of sodium post-treatment<sup>[2,3,50,51]</sup> makes the harmful GBs benign.

### 3.3. CZTS GB with Na and Cu Incorporation

Although anion-core  $\Sigma_3$  (114) GBs of CZTS and CISe have similar atomic structures, their electron charges of the dangling bonds at anion-core atoms are substantively different due to their cation atoms with different valence electrons as shown in Figure 1b (inset). Since there are two S1 atoms (0.50 electron deficiency) with Zn dangling bonds and two S2 atoms (0.25 electron deficiency) with Cu dangling bonds in the unit cell of CZTS GB, 1.50 electrons are needed to satisfy the OEC rule. However, it is impossible to match such fractional charge by doping atoms with integral charge. One needs to double the unit cell of CZTS GB in the GB direction

as the fundamental unit, leaving the integral charges deficiency in this cell. In this case, adding three Na or Cu atoms in X, Y, and Z positions (Figure 1b inset) of double cells CZTS GB (3NaX,Y,Z i or 3CuX,Y,Z i) can completely satisfy the full-shell states of S atoms. Therefore, the following calculations, as we expect, demonstrate the benign electronic structures of 3NaX,Y,Z i and 3CuX,Y,Z i comparing with the prototype GB in CZTS model.

**Figure 5a** shows the band structure and LDOS of  $\Sigma_3$  (114) prototype CZTS GB. We can clearly see that three types of defect states created by the CZTS GB distribute in the band gap, which is consistent with the previous study.<sup>[27]</sup> The shallow defect state below the conduction band minimum (CBM) displays a similar dispersive shape as the lowest conduction band at the gamma point. The LDOS shows that this defect state mainly originates from Cu1 and Sn1 atoms. The localized deep defect state in the center of band gap is extremely det-

imental to the minority carrier lifetime. LDOS shows that it is produced by the antibonding states of S1-S1 dimers (bond length 2.26 Å). The shallow defect states below the valence band maximum level mainly originate from the S2-S2 dimers (bond length 3.11 Å) and Cu2-Sn2 wrong bonds (bond length 2.66 Å). Since the S1-S1 dimers with shorter bond length have stronger coupling than that of S2-S2 dimers, S1-S1 antibonding states give rise to the harmful deep defect levels unoccupied in the band gap.

Na and Cu can really passivate the defect states in CZTS GB by 3NaX,Y,Z i and 3CuX,Y,Z i, which saturate all the unpaired electrons in anion-core as shown in Figure 5b,c. They almost have the same passivation effects from the electronic structures analysis. We can see that most of the defect levels originating from the GB have been removed, and several shallow localized defect states are left in the vicinity of the Fermi energy. From the LDOS, one can see that the deep defect levels created by S1-S1 antibonding states fall down to the near of Fermi level and S2-S2 antibonding states go further to the deep of valence band. The reason is that both of S1-S1 and S2-S2 dimers are substituted by S-Na/Cu pairs with lower energy levels. Meanwhile, the defect state near the CBM created by Cu1-Sn1 wrong bonds goes deeper into the conduction band (not shown in the band structure). Therefore, the Na and Cu passivated CZTS GBs satisfying passivation rule make the solar cells exhibit benign photovoltaic performance.

### 3.4. Formation Energies of CZTS Doped GBs

The relative formation energy  $\Delta H_f^{[45,46]}$  with the Na and Cu incorporated in CZTS prototype GB is defined as

$$\Delta H_f = \Delta E + n_{\text{Cu}}\mu_{\text{Cu}} + n_{\text{Zn}}\mu_{\text{Zn}} + n_{\text{Sn}}\mu_{\text{Sn}} + n_{\text{S}}\mu_{\text{S}} + n_{\text{Na}}\mu_{\text{Na}} \quad (3)$$

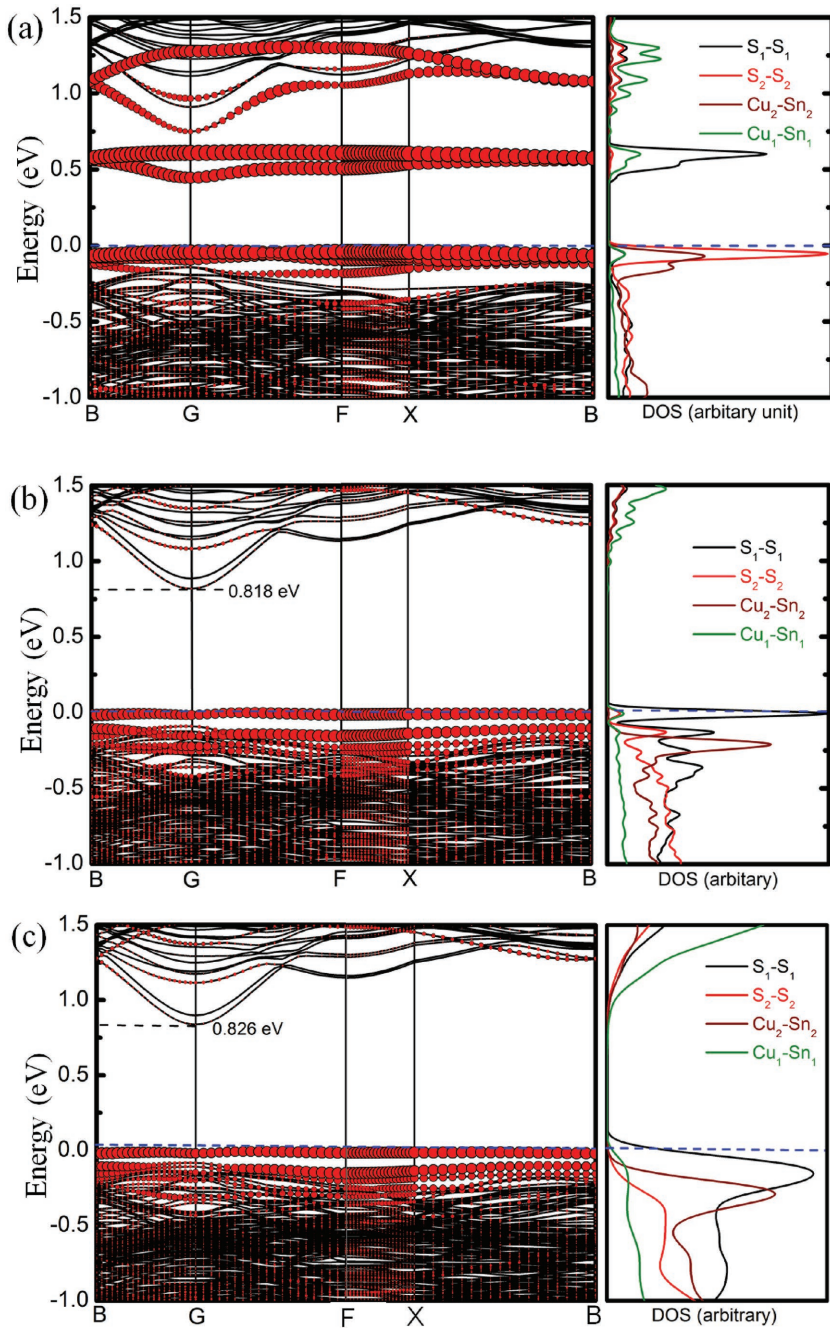


**Figure 5.** Band structures and LDOS of the CZTS GB: a) Prototype GB, b)  $3\text{NaX},\text{Y},\text{Z}$  i, and c)  $3\text{CuX},\text{Y},\text{Z}$  i.  $3\text{NaX},\text{Y},\text{Z}$  i and  $3\text{CuX},\text{Y},\text{Z}$  i doping in CZTS GB clearly shows that the defect levels are removed, leaving a relatively large band gap comparing to the prototype GB (a).

$$\Delta E = E(\text{defect}_{\text{GB}}) - E(\text{prototype}_{\text{GB}}) + n_{\text{Cu}}\mu_{\text{Cu}}^0 + n_{\text{Zn}}\mu_{\text{Zn}}^0 + n_{\text{Sn}}\mu_{\text{Sn}}^0 + n_{\text{S}}\mu_{\text{S}}^0 + n_{\text{Na}}\mu_{\text{Na}}^0 \quad (4)$$

where  $E(\text{prototype}_{\text{GB}})$  is the total energy of prototype GB, which is set as the reference,  $E(\text{defect}_{\text{GB}})$  is the total energy of the GB doped with Cu, Zn, Sn, S, or Na.  $n_{\text{Cu}}$ ,  $n_{\text{Zn}}$ ,  $n_{\text{Sn}}$ ,  $n_{\text{S}}$ , and  $n_{\text{Na}}$  are the numbers of Cu, Zn, Sn, S, and Na atoms referenced to the prototype GB.  $\mu_{\text{Cu}}$ ,  $\mu_{\text{Zn}}$ ,  $\mu_{\text{Sn}}$ ,  $\mu_{\text{S}}$ , and  $\mu_{\text{Na}}$  are the chemical potentials of

Cu, Zn, Sn, S, and Na relative to the chemical potentials  $\mu_{\text{Cu}}^0$ ,  $\mu_{\text{Zn}}^0$ ,  $\mu_{\text{Sn}}^0$ ,  $\mu_{\text{S}}^0$ , and  $\mu_{\text{Na}}^0$  of their elemental phases.

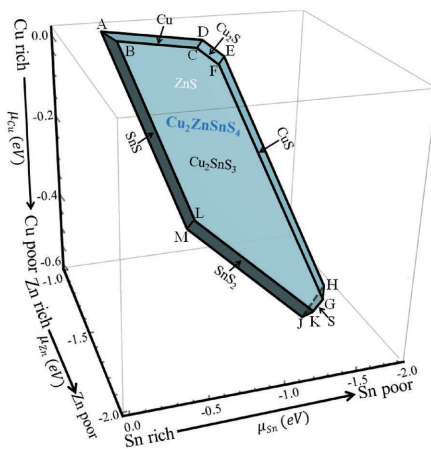
Based on the  $\text{Cu}_2\text{ZnSnS}_4$  stable phase space<sup>[52]</sup> as shown in Figure 6, we considered to avoid the easily formed  $\text{Na}_2\text{S}$  secondary phase and obtained the richest Na chemical region at the intersection points of A, B, C, D, E, F, G, H, J, K, L, and M, whose coordinates are listed in the right of the figure.

According to Equations (3) and (4), we calculated the formation energies of CZTS GBs doped with Na and Cu in X, Y, and Z positions (shown in Figure 1b inset) at the different chemical potentials points shown in Figure 6. Figure 7 shows the formation energies of the Na and Cu doped GBs as a function of the chemical potentials (these values are listed in Table S2, Supporting Information). The fully relaxed atomic structures of these doped GBs are shown in Figure S3 (Supporting Information). From Figure 7, we can see that  $3\text{NaX},\text{Y},\text{Z}$  i not only has lower formation energy than  $3\text{CuX},\text{Y},\text{Z}$  i in all the phase space, but also exhibits more stable structure than the prototype GB in most of the chemical potential regions, excepting a few points (G, H, J, and F). These indicate that Na segregating in GB is more feasible than Cu in CZTS system. Furthermore, it can spontaneously segregate at the CZTS GBs to passivate GB defect states.

#### 4. Conclusions

We showed that the deep-level states of the unpassivated GBs of CISe and CZTS can be passivated by Na and Cu based on the self-passivation rule. Na can not only cleanly passivate the GB defect states, but also has negative formation energies in these systems, which indicate that Na prefers to segregate at the GBs in agreement with the available experiments. Cu can also self-passivate the GB defect states in CISe and CZTS under Cu rich conditions. However, to obtain the desired concentration of Cu vacancies and the hole carriers in interior grains, a Cu poor synthesis condition is usually necessary, so one cannot use Cu to passivate defect states

in such compounds. Therefore, Na post-treatment becomes the best approach to passivate the GB defect states. In fact, we have also demonstrated that other types of atoms, such as Ca which satisfies the passivation rule, can also completely eliminate GB defect states. The present work not only provides a mechanism explaining why sodium treatment is used to enhance the photovoltaic efficiencies through passivating the GB defect states, but also the proposed passivation method can be applied



	$\mu_{Cu}$ (eV)	$\mu_{Zn}$ (eV)	$\mu_{Sn}$ (eV)	$\mu_S$ (eV)	$\mu_{Na}$ (eV)
A:	( 0.000	-1.025	-0.285	-0.725	-1.579)
B:	( 0.000	-1.175	-0.335	-0.675	-1.604)
C:	( 0.000	-1.330	-0.800	-0.520	-1.681)
D:	( 0.000	-1.230	-0.900	-0.520	-1.681)
E:	( -0.030	-1.290	-1.020	-0.460	-1.711)
F:	( -0.030	-1.390	-0.920	-0.460	-1.711)
G:	( -0.490	-1.900	-1.330	0.000	-1.941)
H:	( -0.490	-1.750	-1.480	0.000	-1.941)
J:	( -0.565	-1.750	-1.330	0.000	-1.941)
K:	( -0.515	-1.850	-1.330	0.000	-1.941)
L:	( -0.355	-1.530	-0.690	-1.280	-1.301)
M:	( -0.405	-1.430	-0.690	-1.280	-1.301)

**Figure 6.** The calculated stable chemical potential region of CZTS phase diagram with the consideration of avoiding the easily formed  $Na_2S$  secondary phase ( $2\mu_{Na} + \mu_S \leq \Delta H_f (Na_2S) = -3.882$  eV). The corresponding coordinates for the upper limitation of richest Na chemical potential at the points A, B, C, D, E, F, G, H, J, K, L, and M are shown in the right of the figure.

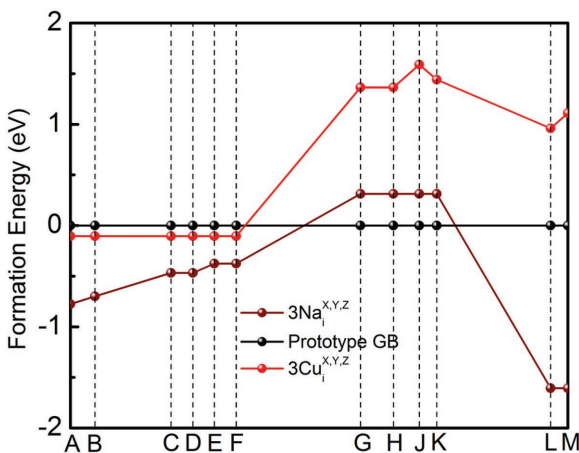


**Figure 7.** The formation energies of anion-core CZTS GB structures doped with Na and Cu at the selected points in the stable chemical potential region (shown in Figure 6).  $3NaX,Y,Z$  i does not only have lower formation energy than  $3CuX,Y,Z$  i, but also spontaneously segregates at GBs with negative formation energies in almost all the phase space.

to other semiconductor compounds, such as CdTe, GaAs, and  $CH_3NH_3PbI_3$  ( $AB_3$ ).

## Supporting Information

Supporting Information is available from the Wiley Online Library or from the author.

## Acknowledgements

The authors greatly thank the stimulating discussion with Prof. Su-Huai Wei and Dr. Yu-Sheng Hou. This work was partially supported by the Special Funds for Major State Basic Research (2016YF0700701), National Science Foundation of China (NSFC), International Collaboration Project of Shanghai Municipality, Pujiang plan, Program for Professor of Special Appointment (Eastern Scholar), Shanghai Rising-star program, Qing Nian Ba Jian Program, and Fok Ying Tung Education Foundation.

Computation was performed in the Supercomputer Center of Fudan University. S.-Y.C. was supported by NSFC under grant no. 61574059, Shu-Guang program, and CC of ECNU.

Received: July 5, 2016

Revised: October 26, 2016

Published online: December 21, 2016

- [1] D. Rudmann, G. Bilger, M. Kaelin, F.-J. Haug, H. Zogg, A. N. Tiwari, *Thin Solid Films* **2003**, 431, 37.
- [2] D. Rudmann, A. F. D. Cunha, M. Kaelin, F. Kurdesau, H. Zogg, A. N. Tiwari, G. Bilger, *Appl. Phys. Lett.* **2004**, 84, 1129.
- [3] D. Rudmann, D. Brémaud, H. Zogg, A. N. Tiwari, *J. Appl. Phys.* **2005**, 97, 084903.
- [4] D. Rudmann, D. Brémaud, A. F. D. Cunha, G. Bilger, A. Strohm, M. Kaelin, H. Zogg, A. N. Tiwari, *Thin Solid Films* **2005**, 480, 55.
- [5] P. Jackson, R. Wuerz, D. Hariskos, E. Lotter, W. Witte, M. Powalla, *Phys. Status Solidi RRL* **2016**, 8, 583.
- [6] M. B. Ård, K. Granath, L. Stolt, *Thin Solid Films* **2000**, 361, 9.
- [7] H. Zhou, T. B. Song, W. C. Hsu, S. Lou, S. Ye, H. S. Duan, C. J. Hsu, W. Yang, Y. Yang, *J. Am. Chem. Soc.* **2013**, 135, 15998.
- [8] K. Granath, M. Bodegård, L. Stolt, *Sol. Energy Mater. Sol. Cells* **2000**, 60, 279.
- [9] T. Gershon, B. Shin, N. Bojarczuk, M. Hopstaken, D. B. Mitzi, S. Guha, *Adv. Energy Mater.* **2015**, 5, 1400849.
- [10] A. Nagaoka, H. Miyake, T. Taniyama, K. Kakimoto, Y. Nose, M. A. Scarpulla, K. Yoshino, *Appl. Phys. Lett.* **2014**, 104, 152101.
- [11] L. Stolt, J. Hedström, J. Kessler, M. Ruckh, K.-O. Velthaus, H.-W. Schock, *Appl. Phys. Lett.* **1993**, 62, 597.
- [12] M. R. Byeon, E. H. Chung, J. P. Kim, T. E. Hong, J. S. Jin, E. D. Jeong, J. S. Bae, Y. D. Kim, S. Park, W. T. Oh, Y. S. Huh, S. J. Chang, S. B. Lee, I. H. Jung, J. Hwang, *Thin Solid Films* **2013**, 546, 387.
- [13] R. Wuerz, A. Eicke, F. Kessler, P. Rogin, O. Y. Assl, *Thin Solid Films* **2011**, 519, 7268.
- [14] P. Blösch, S. Nishiwaki, A. Chirilă, L. Kranz, C. Fella, F. Pianezzi, C. Adelhelm, E. Franzke, S. Buecheler, A. N. Tiwari, *Thin Solid Films* **2013**, 535, 214.
- [15] J. H. Yun, K. H. Kim, M. S. Kim, B. T. Ahn, S. J. Ahn, J. C. Lee, K. H. Yoon, *Thin Solid Films* **2007**, 515, 5876.
- [16] M. A. Green, K. Emery, Y. Hishikawa, W. Warta, E. E. Dunlop, *Prog. Photovolt: Res. Appl.* **2015**, 23, 1.

- [17] M. Bodegård, L. Stolt, J. Hedström, in *12th European Photovoltaic Solar Energy Conference* (Eds: R. Hill, W. Palz, P. Helm), Stephens, Bedford **1994**, pp. 236–239.
- [18] D. Braunger, D. Hariskos, G. Bilger, U. Rau, H. W. Schock, *Thin Solid Films* **2000**, *361*, 161.
- [19] M. Johnson, S. V. Baryshev, E. Thimsen, M. Manno, X. Zhang, I. V. Veryovkin, C. Leighton, E. S. Aydil, *Energy Environ. Sci.* **2014**, *7*, 1931.
- [20] C. S. Jiang, R. Noufi, K. Ramanathan, J. A. Abushama, H. R. Moutinho, M. M. A. Jassim, *Appl. Phys. Lett.* **2004**, *85*, 2625.
- [21] C. S. Jiang, R. Noufi, J. A. Abushama, K. Ramanathan, H. R. Moutinho, J. Pankow, M. M. A. Jassim, *Appl. Phys. Lett.* **2004**, *84*, 3477.
- [22] Y. Yan, C.-S. Jiang, R. Noufi, S.-H. Wei, H. R. Moutinho, M. M. A. Jassim, *Phys. Rev. Lett.* **2007**, *99*, 235504.
- [23] S. Tajima, R. Asahi, D. Isheim, D. N. Seidman, T. Itoh, K.-I. Ohishi, *Jpn. J. Appl. Phys.* **2015**, *54*, 112302.
- [24] H. Mirhosseini, J. Kiss, C. Felser, *Phys. Rev. Appl.* **2015**, *4*, 064005.
- [25] J. Li, D. B. Mitzi, V. B. Shenoy, *ACS Nano* **2011**, *5*, 8613.
- [26] W.-J. Yin, Y. Wu, R. Noufi, M. A. Jassim, Y. Yan, *Appl. Phys. Lett.* **2013**, *102*, 193905.
- [27] W.-J. Yin, Y. Wu, S. H. Wei, R. Noufi, M. M. A. Jassim, Y. Yan, *Adv. Energy Mater.* **2014**, *4*, 1300712.
- [28] Y. Yan, W.-J. Yin, Y. Wu, T. Shi, N. R. Paudel, C. Li, J. Poplawsky, Z. Wang, J. Moseley, H. Guthrey, H. Moutinho, S. J. Pennycook, M. M. A. Jassim, *J. Appl. Phys.* **2015**, *117*, 112807.
- [29] S.-H. Wei, S. B. Zhang, A. Zunger, *J. Appl. Phys.* **1999**, *85*, 7214.
- [30] Z. Y. Zhao, X. Zhao, *Inorg. Chem.* **2014**, *53*, 9235.
- [31] L. E. Oikkonen, M. G. Ganchenkova, A. P. Seitsonen, R. M. Nieminen, *J. Appl. Phys.* **2013**, *114*, 083503.
- [32] Y. Yan, M. M. A. Jassim, K. M. Jones, *J. Appl. Phys.* **2003**, *94*, 2976.
- [33] C.-Y. Liu, Y.-Y. Zhang, Y.-S. Hou, S.-Y. Chen, H.-J. Xiang, X.-G. Gong, *Phys. Rev. B* **2016**, *93*, 205426.
- [34] P. Koskinen, S. Malola, H. Hakkinen, *Phys. Rev. Lett.* **2008**, *101*, 115502.
- [35] M. C. Lucking, J. Bang, H. Terrones, Y.-Y. Sun, S. Zhang, *Chem. Mater.* **2015**, *27*, 3326.
- [36] S. Iarlori, G. Galli, F. Gygi, M. Parrinello, E. Tosatti, *Phys. Rev. Lett.* **1992**, *69*, 2947.
- [37] Q. Wang, A. R. Oganov, Q. Zhu, X.-F. Zhou, *Phys. Rev. Lett.* **2014**, *113*, 266101.
- [38] H.-X. Deng, S.-S. Li, J. Li, S.-H. Wei, *Phys. Rev. B* **2012**, *85*, 195328.
- [39] G. Kresse, J. Hafner, *Phys. Rev. B* **1993**, *47*, 558.
- [40] G. Kresse, J. Hafner, *Phys. Rev. B* **1994**, *49*, 14251.
- [41] G. Kresse, D. Joubert, *Phys. Rev. B* **1999**, *59*, 1758.
- [42] J. P. Perdew, Y. Wang, *Phys. Rev. B* **1992**, *45*, 13244.
- [43] S. L. Dudarev, G. A. Botton, S. Y. Savrasov, C. J. Humphreys, A. P. Sutton, *Phys. Rev. B* **1998**, *57*, 1505.
- [44] H. J. Monkhorst, J. D. Pack, *Phys. Rev. B* **1976**, *13*, 5188.
- [45] S. Chen, J.-H. Yang, X. G. Gong, A. Walsh, S.-H. Wei, *Phys. Rev. B* **2010**, *81*, 245204.
- [46] B. Liu, Z. Qi, C. Shi, *Phys. Rev. B* **2006**, *74*, 174101.
- [47] C. Persson, A. Zunger, *Phys. Rev. Lett.* **2003**, *91*, 266401.
- [48] S. Chen, X. G. Gong, A. Walsh, S.-H. Wei, *Appl. Phys. Lett.* **2010**, *96*, 021902.
- [49] S.-H. Han, A. M. Hermann, F. S. Hasoon, H. A. A. Thani, D. H. Levi, *Appl. Phys. Lett.* **2004**, *85*, 576.
- [50] O. C. Mirédin, P. Choi, R. Wuerz, D. Raabe, *Ultramicroscopy* **2011**, *111*, 552.
- [51] D. Braunger, D. Hariskos, G. Bilger, U. Rau, H. W. Schock, *Thin Solid Films* **2000**, *361*, 161.
- [52] S. Chen, J.-H. Yang, X. G. Gong, A. Walsh, S.-H. Wei, *Phys. Rev. B* **2010**, *81*, 245204.